GEOPHYSICS, VOL. 63, NO. 5 (SEPTEMBER-OCTOBER 1998); P. 1604–1617, 10 FIGS., 7 TABLES.

Seismic monitoring of a CO_2 flood in a carbonate reservoir: A rock physics study

Zhijing Wang*, Michael E. Cates*, and Robert T. Langan*

ABSTRACT

A carbon dioxide (CO_2) injection pilot project is underway in Section 205 of the McElroy field, West Texas. High-resolution crosswell seismic imaging surveys were conducted before and after CO_2 flooding to monitor the CO_2 flood process and map the flooded zones. The velocity changes observed by these time-lapse surveys are typically on the order of −6%, with maximum values on the order of −10% in the vicinity of the injection well. These values generally agree with laboratory measurements if the effects of changing pore pressure are included.

The observed dramatic compressional (V_P) and shear (V_S) velocity changes are considerably greater than we had initially predicted using the Gassmann (1951) fluid substitution analysis (Nolen-Hoeksema et al., 1995) because we had assumed reservoir pressure would not change from survey to survey. However, the post-CO_2 reservoir pore fluid pressure was substantially higher than the original pore pressure. In addition, our original petrophysical data for dry and brine-saturated reservoir rocks did not cover the range of pressures actually seen in the field. Therefore, we undertook a rock physics study of CO_2 flooding in the laboratory, under the simulated McElroy pressures and temperature.

Our results show that the combined effects of pore pressure buildup and fluid substitution caused by CO_2 flooding make it petrophysically feasible to monitor the CO_2 flood process and to map the flooded zones seismically. The measured data show that V_P decreases from a minimum 3.0% to as high as 10.9%, while V_S decreases from 3.3% to 9.5% as the reservoir rocks are flooded with CO_2 under in-situ conditions. Such V_P and V_S decreases, even if averaged over all the samples measured, are probably detectable by either crosswell or high-resolution surface seismic imaging technologies.

Our results show V_P is sensitive to both the CO_2 saturation and the pore pressure increase, but V_S is particularly sensitive to the pore pressure increase. As a result, the combined V_P and V_S changes caused by the CO_2 injection may be used, at least semiquantitatively, to separate CO_2-flooded zones with pore pressure buildup from those regions without pore pressure buildup or to separate CO_2 zones from pressured-up, non-CO_2 zones.

Our laboratory results show that the largest V_P and V_S changes caused by CO_2 injection are associated with high-porosity, high-permeability rocks. In other words, CO_2 flooding and pore pressure buildup decrease V_P and V_S more in high-porosity, high-permeability samples. Therefore, it may be possible to delineate such high-porosity, high-permeability streaks seismically in situ. If the streaks are thick enough compared to seismic resolution, they can be identified by the larger V_P or V_S changes.

INTRODUCTION

The McElroy Field is located on the eastern margin of the central basin platform in Crane and Upton counties, Texas. The reservoir is approximately 2900 ft (884 m) deep (below surface) in the Permian Grayburg Formation. Oil production, which started in the late-1920s, comes from a gross pay zone that averages 275 ft (84 m) thick. The reservoir rock is composed of dolostones with variable amounts of evaporite cement (mostly gypsum). Porosity and permeability vary greatly both vertically and horizontally. Such heterogeneities are caused mainly by secondary porosity and evaporite cementation. The average porosity in the reservoir is around 10%. Permeability varies from less than 0.01 millidarcy (md) (0.01×10^{-11} cm^2) to as

Manuscript received by the Editor November 4, 1996; revised manuscript received January 12, 1998.
*Chevron Petroleum Technology Company, P.O. Box 446, La Habra, California 90633-0446; E-mail: zwan@chevron.com, mcat@chevron.com, rtlr@chevron.com.

high as 90 md (90×10^{-11} cm^2). As a result of reservoir heterogeneity, oil recovery efficiency varies dramatically throughout the reservoir (Harris et al., 1995).

The reservoir oil is around 34° API (bulk density is approximately 0.85 g/cm^3 at 16°C and 1 atm). The reservoir had been waterflooded, and at the time of CO_2 injection, the saturation in the reservoir was estimated to be on average 50% water and 50% oil.

A series of high-resolution crosswell seismic surveys conducted by the McElroy Reservoir Geosciences Project (MRGP) in the McElroy 205 CO_2 pilot area have detected substantial changes in both V_P and V_S in the reservoir, attributable to the injection of CO_2. The baseline or reference surveys were conducted in 1993 during waterflooding and before the commencement of CO_2 injection. The post-CO_2 surveys were conducted in August 1995 about 10 months after CO_2 injection had resumed in the pilot (there had been a one-year hiatus because of CO_2 supply problems). The velocity changes observed by these time-lapse surveys are typically −6%, with maximum values on the order of −10% in the vicinity of the injection well (Lazaratos and Marion, 1996).

Figure 1 shows the compressional velocity (V_P) changes recorded by crosswell tomographic seismic imaging. In the injection well (well 1068), V_P decreases by over 1000 ft/s (305 m/s) in a 200-ft section. Since the original V_P before CO_2 flooding is around 16 600 ft/s (5060 m/s), a V_P change of 1000 ft/s (305 m/s) is equivalent to 6%. Most of the V_P decreases are confined to the reservoir section and the immediate vicinity beneath the reservoir.

These changes in velocity are attributable to changes in both CO_2 saturation and pore pressure. At the time the baseline survey was collected, the measured bottom-hole pore pressure was about 1200 psi (8.3 MPa). At the time of the post-CO_2 survey, the measured bottom-hole pore pressure was as high as 2300 psi (15.9 MPa), resulting in a decrease in differential pressure of 1100 psi (7.6 MPa) near the borehole.

The observed V_P and shear (V_S) velocity changes are considerably greater than we had predicted using the Gassmann (1951) fluid substitution analysis based on laboratory measured petrophysical properties and velocities in dry rocks (Nolen-Hoeksema et al., 1995). This is because initially we had applied the Gassmann relationship assuming the reservoir pressures would not change from survey to survey, which was incorrect. In addition, our original petrophysical data for dry and brine-saturated reservoir rocks did not cover the range of pressures actually seen in the field. Therefore, we selected eight core samples from the same reservoir section of the same well (number 1202) as those used by Nolen-Hoeksema et al. (1995) and

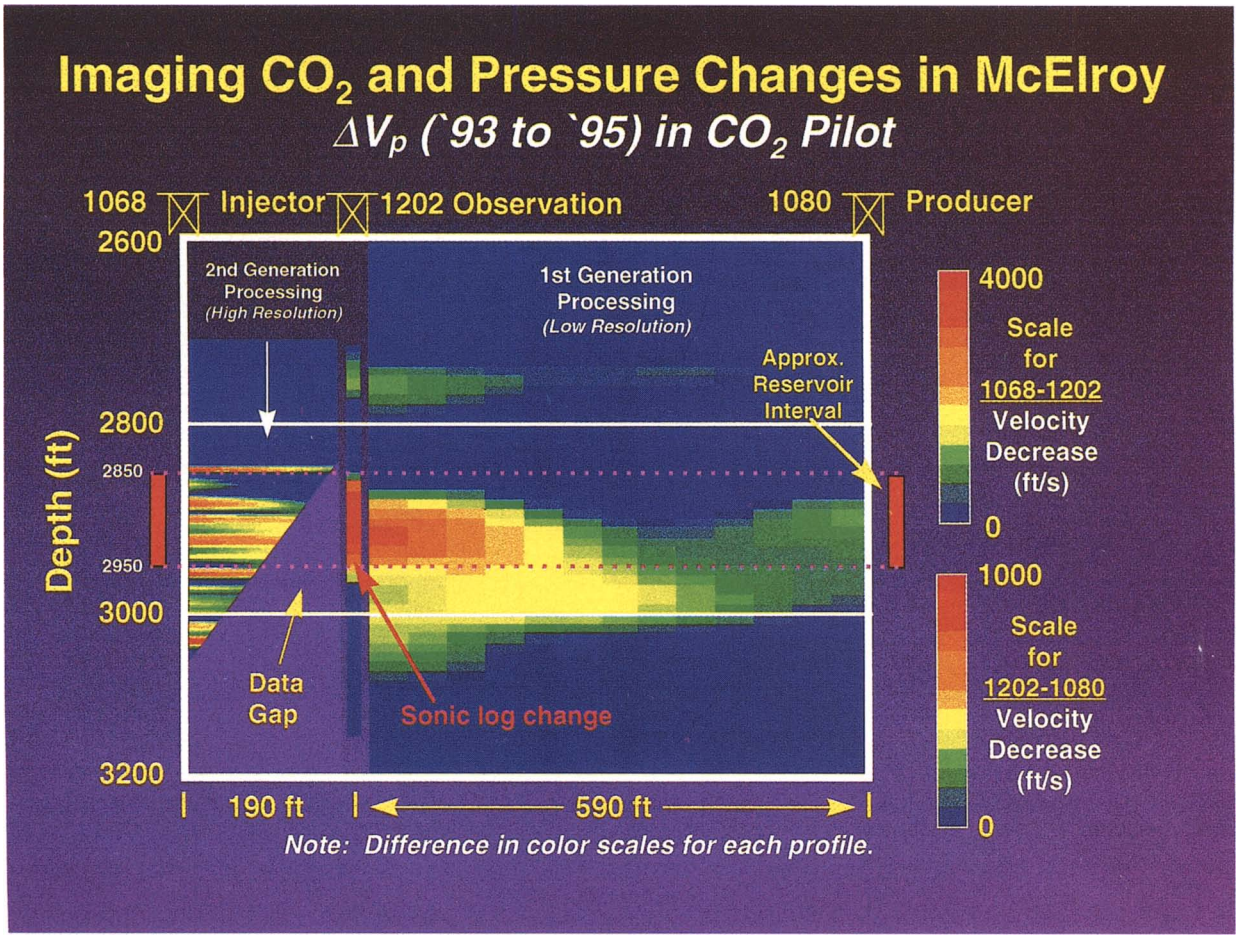

FIG. 1. Tomographic image of V_P difference between 1995 monitor survey and 1993 baseline survey. V_P decreases more than 1000 ft/s (305 m/s) or 6% near the injector (well 1068). Away from the injector, most V_P decreases are confined to the reservoir section.

undertook a laboratory study of CO_2 flooding, duplicating the in-situ McElroy reservoir pressures and temperature.

The main objective of this laboratory study is to help interpret the crosswell seismic data. Our laboratory results show that the combined effects of CO_2 saturation and pore pressure increase from CO_2 injection decrease V_P by as much as 11%, with an average decrease of about 6%, and the V_S by as much as 10%, with an average decrease of 5%.

LABORATORY MEASUREMENTS

Sample selection and petrophysical properties

A section of 283 ft (86 m) of dolostone was cored from the number 1202 well (from the interval of 2778 to 3061 ft). The cores have a diameter of 3.5 in. (8.9 cm) and were slabbed at one-third of the diameter for core photography and descriptions. A core analysis plan was laid out specifically to measure acoustic/seismic velocities for correlating velocity-lithology/porosity and for the feasibility study of seismic monitoring of the CO_2 flood in this reservoir using crosswell seismic imaging.

We selected eight core samples for analysis on the effects of CO_2 saturation and pore pressure change on velocity. Since the cores were slabbed, velocity measurements on full-diameter cores were impossible, so plugs of 1.5 in. (3.8 cm) diameter were drilled. These cores were from the same well as those analyzed by Nolen-Hoeksema et al. (1995). The eight core plugs were selected to represent reservoir rocks of various porosities (from 7.9% to 22.1%) and permeability (from 0.07 md to 66.7 md). We included one sample (sample 12) from the relatively high-porosity unit immediately below the reservoir. The lengths of the plugs varied from 1.5 to 2.0 inches (3.8 to 5.1 cm).

The core plugs were cleaned by a low-temperature solvent extraction method to prevent dissolving the gypsum cement filling some of the pores. We measured porosity, permeability, and grain density at ambient temperature and pressure. These measured petrophysical properties, along with the depth, depositional environment, and texture, are listed in Table 1.

Seismic properties

V_p and shear V_S wave velocities were measured on all eight core samples at different net overburden pressures (net overburden pressure is the difference between the overburden pressure and pore fluid pressure, sometimes called differential or effective pressure). Before the velocity measurements, the core samples were dried in a vacuum oven at about 22°C for at least 72 hours. Low-temperature drying prevents thermally cracking the cores.

Once a core sample was prepared, it was jacketed in a corrosion-resistant plastic sleeve with acoustic transducers, one transmitting and one receiving, and fitted into a pressure vessel of constant temperature (88°F or 31°C) equal to the McElroy reservoir temperature. Both compressional and shear waves of about 500 kHz frequency were propagated into the sample with the transmitting transducer. After traveling through the sample, the wave energy was picked up by the receiving transducer and recorded by a controlling computer. Transducers were calibrated over the pressure and temperature range using standard reference materials and face to face. Changes in sample length were precisely measured during experiments. The velocities of both compressional and shear waves through the rock sample were thus deduced accurately. Our estimates of the uncertainty in the measured velocities are <0.5% for V_P and <1% for V_S. All the measurements were done at a constant 88°F (31°C).

Our experimental procedure for seismic property measurements is as follows:

1) Both V_P and V_S were measured in the air-saturated (dry) sample at overburden pressures of 300, 600, 900, 1300, and 1700 psi (2.1, 4.1, 6.2, 9.0, and 11.7 MPa), respectively, and zero pore pressure.
2) After the dry velocities were measured, the core remained inside the pressure vessel and was evacuated to about 5 μm mercury. A pure hydrocarbon oil (Carnation), which has properties (density, viscosity, and compressibility) similar to the reservoir oil, was injected into the core for 15 to 110 hours, depending on the sample's permeability, at a pore pressure of 1200 psi (8.3 MPa) and overburden pressure of 2900 psi (20 MPa).
3) The sample was flooded with water at a constant pore pressure and a constant back pressure of 1200 psi (8.3 MPa). The pressure drop across the sample ranged from a few psi to as high as 600 psi, depending on the sample's permeability. The flow rate of waterflooding was about 2 cm^3/hour. Approximately 10 pore volumes of water flowed through the sample. The total amount of fluid displaced was recorded by both the displacing and backing digital pumps. The amount of oil displaced from the core sample was measured to calculate oil/water saturation of the sample after waterflood. The oil and water saturation of the samples was on average about 60% and 40%, respectively. After CO_2 flood, V_P and V_S were measured again in the same sample at a constant overburden pressure of 2900 psi (20 MPa) and various pore pressures of 1200, 1600, 2000, 2300, and 2600 psi (8.3, 11.0, 13.8, 15.9, and 17.9 MPa), respectively.
4) The sample was finally flooded with CO_2 at constant pore and back pressures. The procedure for CO_2 flooding was essentially the same as for waterflooding. V_P and V_S were measured in the same sample, which was flooded

Table 1. Petrophysical properties of selected cores.

Sample number	Depth (ft)	Depth (m)	Porosity (%)	Permeability (md)	Grain density (g/cm^3)	Depositional environment	Depositional facies/texture
1	2794.1	851.64	12.0	1.08	2.85	Intertidal	Peloid dolopackstone
5	2865.1	873.28	21.4	53.10	2.84	Shallow marine	Peloid dolopackstone
6	2887.1	879.99	21.7	53.90	2.85	Shallow marine	Fusulinid peloid dolowackestone
7	2907.9	886.33	13.7	16.90	2.79	Shallow marine	Brachiopod peloid dolopackstone
8	2911.8	887.52	22.1	66.70	2.85	Shallow marine	Brachiopod peloid dolopackstone
9	2928.9	892.73	12.3	2.56	2.78	Shallow marine	Peloid dolopackstone
11	2951.9	899.74	7.9	0.40	2.83	Open marine	Peloid dolopackstone
12	2997.1	913.52	8.2	0.07	2.78	Open marine	Fusulinid peloid dolowackestone

with CO_2 at a constant overburden pressure of 2900 psi (20 MPa) and various pore pressures. Final oil/water/CO_2 saturation was estimated by the sample weights at different saturations.

The complete suite of measurements described above took 7 to 14 days for each core sample.

Figure 2 shows, as an example, the recorded compressional (Figure 2a) and shear (Figure 2b) waves in sample 5 saturated with air at different pressures (for clarity, only three of the five waveforms are plotted here). As the net overburden pressure increases, the traveltimes decrease and amplitudes increase for both *P*- and *S*-waves. Figure 3 shows the compressional (Figure 3a) and shear (Figure 3b) waves in the same sample with various fluids at a net overburden pressure of 1700 psi (11.7 MPa). As the gas (air) in the pores is replaced by oil/water (about 60/40), traveltimes decrease and amplitudes increase for the *P*-wave while the *S*-wave shows the opposite because *P*-waves are less, whereas *S*-waves are more, attenuative in liquid-saturated rocks than in gas-saturated rocks. After the oil/water-saturated sample is flooded with CO_2, traveltimes increase and amplitudes decrease for the *P*-wave, while the *S*-wave is hardly affected.

RESULTS

Properties of reservoir fluids

Four fluids were involved in the experiments: air, water, oil, and CO_2. Because of air's high compressibility and low density, its saturation effect on seismic velocities in a dry rock with empty pores usually is negligible at zero pore pressure. The formation brine in the McElroy Field has a density of 1.023 g/cm^3. The amount of total dissolved solids in the brine is around 41,500 ppm, most of which is NaCl. Figure 4 shows the velocity and bulk modulus of a similar formation brine (Batzle and Wang, 1992) versus pressure at reservoir temperature (31°C). Both V_P and bulk modulus increase approximately linearly with increasing pressure.

The Carnation oil is a hydrocarbon (paraffin) oil that has essentially the same properties (API gravity, viscosity, velocity) as the produced reservoir oil from the McElroy Field. It was used to simulate the reservoir oil because of its nontoxicity, ease of handling, and known seismic properties. It is also miscible with CO_2 under McElroy reservoir conditions. Figure 4 also shows the velocity and bulk modulus of the Carnation oil measured by Wang et al. (1991). Both V_P and bulk modulus of

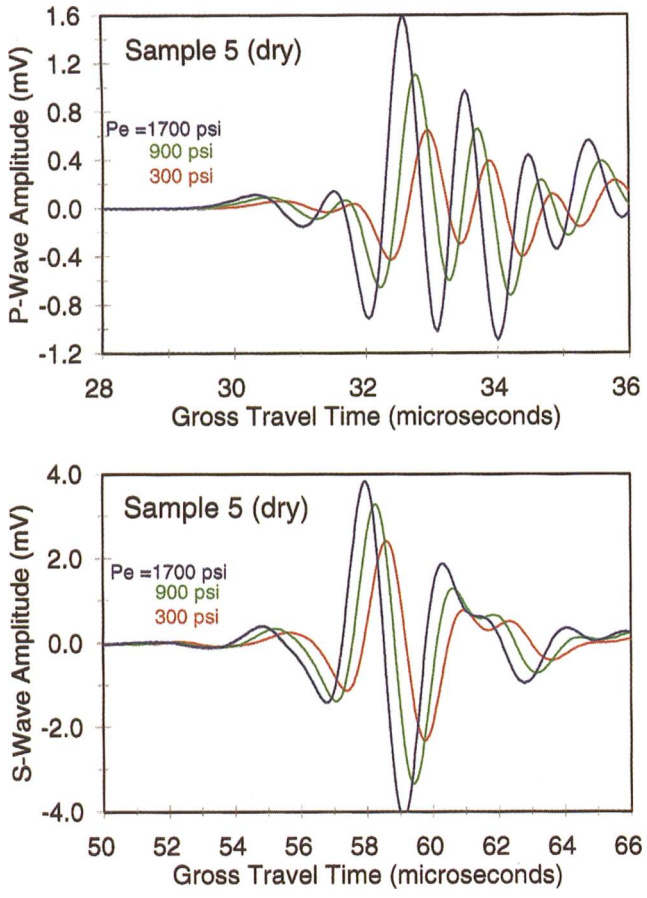

FIG. 2. Example of compressional (a) and shear (b) waves in gas-saturated sample 5 at three net overburden pressures (Pe). As the net overburden pressure increases, traveltime decreases and amplitude increases for both *P*- and *S*-waves.

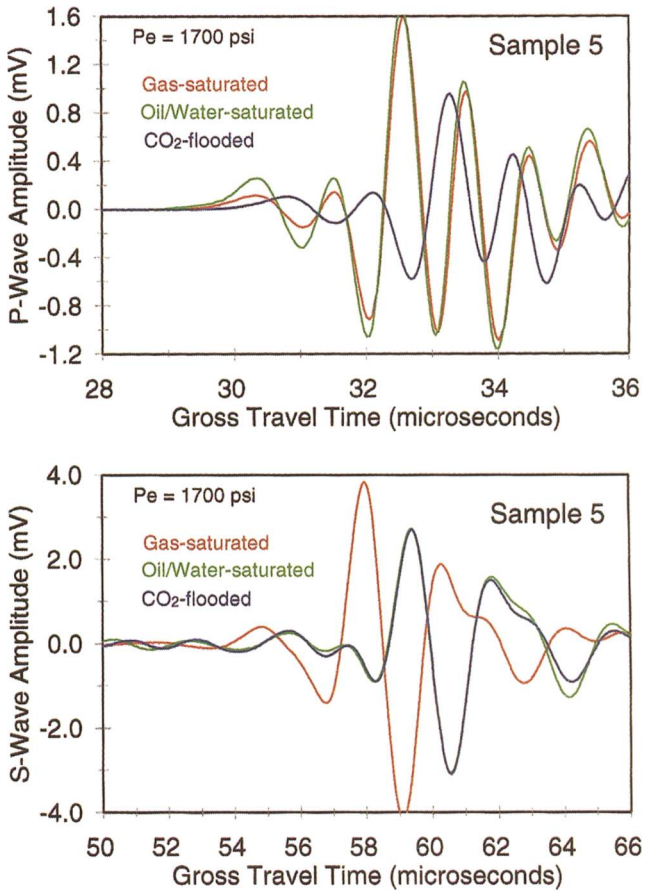

FIG. 3. Example of compressional (a) and shear (b) waves in sample 5 at three saturation states: gas saturated (dry), oil/water (55/45%) saturated, and CO_2 flooded (76% CO_2 and 24% oil and water). As the oil/water-saturated sample is flooded with CO_2, traveltime increases and amplitude decreases for the *P*-wave while the *S*-wave hardly changes.

the oil are substantially lower than those of water at reservoir temperature.

The CO_2 with purity >99.5% was obtained from a commercial source. Its critical point is 31°C (88°F) at 7.4 MPa (1070 psi). Above the critical temperature, CO_2 behaves like a gas. Below the critical temperature and above the critical pressure, CO_2 is a liquid.

Figures 5a and 5b show the velocity, bulk modulus, and bulk density of CO_2 at 30°C (86°F) versus pressure. These properties were measured at a temperature 1°C below the McElroy reservoir temperature because of measurement difficulties at the critical temperature point.

In general, CO_2 has dramatically different properties from either water or oil (Wang and Nur, 1989). At the pre-CO_2 McElroy reservoir conditions (pore pressure = 1200 psi and temperature = 88°F), its bulk modulus is only about 3% but its density is almost 60% of water's. At high injection pressures, CO_2's density approaches water density, but its bulk modulus remains considerably below that of water. For example, at a pore pressure of 2300 psi (15.9 MPa), CO_2's density is 86.5% of water's density, but its bulk modulus is less than 10% of water's bulk modulus. Therefore, CO_2 at this pressure and temperature can be considered a highly compressible liquid. Furthermore, the CO_2 properties change rapidly with pressure for pressures between 1070 and 1500 psi (7.4 and 10.3 MPa).

At the McElroy reservoir temperature, CO_2 is a gas when the reservoir pore pressure is lower than approximately 1000 psi (6.9 MPa) and a liquid when the reservoir pore pressure is above 1000 psi. The compressional velocity in the CO_2 gas phase decreases as pressure increases because density increases faster than the bulk modulus. In liquid CO_2, velocity increases with increasing pressure. Figure 5b shows the rapid increase in bulk density of CO_2 as pressure increases, especially in the pressure range from 1000 psi (6.9 MPa) to 2000 psi (13.8 MPa).

Efficiency of water displacement and CO_2 flooding

Table 2 shows the detailed fluid displacement and saturation information for each of the measured samples. In the table, the pore volume of a sample was measured using helium porosimetry. The injected fluids (water or CO_2) were tabulated in terms of absolute volume and pore volume. The amount of oil displaced during water injection was measured by separating it from water. After the water displacement, oil and water saturations were calculated by

$$\text{Oil saturation} = \frac{\text{Pore volume} - \text{Volume of displaced oil}}{\text{Pore volume}} \times 100\% \quad (1)$$

and

$$\text{Water saturation} = 100 - \text{Oil saturation}\,(\%). \quad (2)$$

The final CO_2 saturation of the sample after CO_2 flooding was estimated using the final weight of the sample by assuming that all CO_2 inside the sample had evaporated at room conditions after the sample had sat in a fume hood for two to three

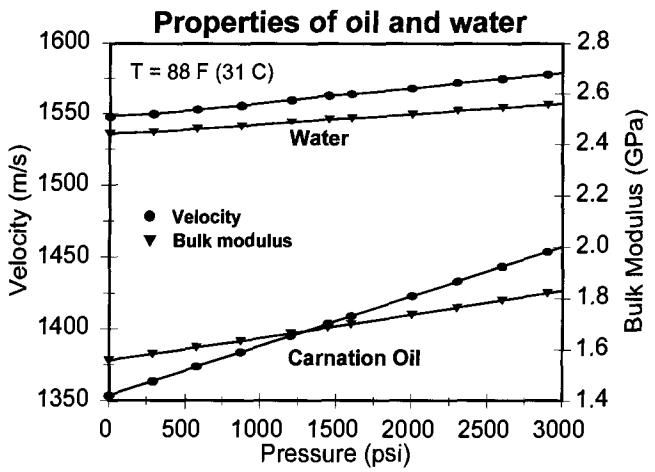

FIG. 4. Velocities (left y-axis) and bulk moduli (right y-axis) versus pressure in formation water and oil. The properties of formation water and Carnation oil are similar to those of McElroy formation brine and oil, respectively. Both velocity and bulk modulus increase as pressure increases.

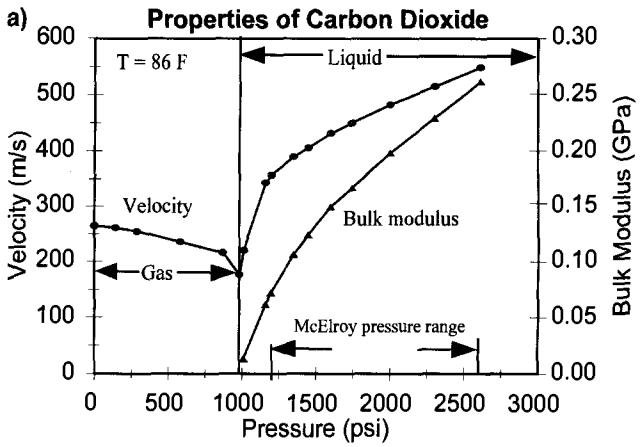

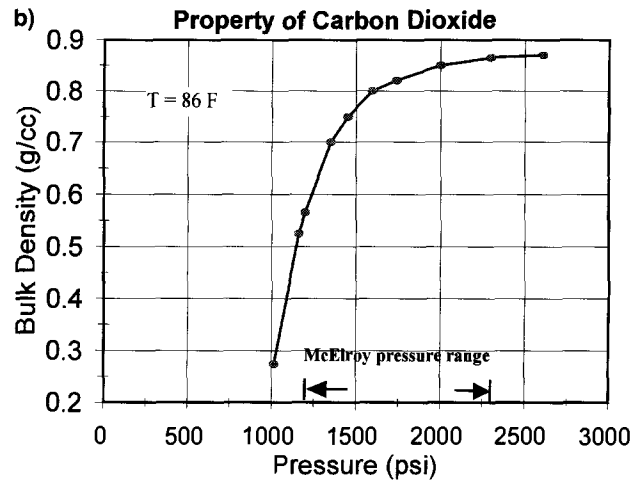

FIG. 5. Velocities (left y-axis), bulk moduli (right y-axis) (a), and bulk density (b) versus pressure in CO_2 at 86°F (30°C). The CO_2 density can be very close to, but its bulk modulus is less than 10% of, those of the McElroy reservoir fluids (oil/water) under reservoir condition.

days.

$$\text{Final oil/water saturation} = \frac{\text{Final sample weight} - \text{Dry sample weight}}{\text{Oil/water density} \times \text{Pore volume}} \times 100\% \quad (3)$$

and

$$\text{Final } CO_2 \text{ saturation} = 100 - \text{Final oil/water saturation}\,(\%). \quad (4)$$

Table 2 shows that CO_2 injection on average has a flood efficiency of about 63%. We therefore estimate the final average oil/water saturation of the sample to be around 37%. Because of facility limitations, we did not attempt to separate the final saturation into oil saturation and water saturation. Saturations presented in Table 2 are approximate within ±5% of the saturation unit because of the small pore volumes of the samples and the assumption that only CO_2 evaporated from the finished core samples (oil did not evaporate in 2 to 3 days).

Velocity versus porosity

As shown in Nolen-Hoeksema et al. (1995), seismic velocities in the San Andres/Grayburg formations of the McElroy field decrease approximately linearly with increasing porosity. Figure 6a shows V_P and V_S versus porosity in the measured dry samples (saturated with air) at the original (before CO_2 flooding) reservoir effective pressure and temperature. Both V_P and V_S decrease linearly with increasing porosity as represented by the following empirical fits to the data:

$$V_P = 6101 - 63.98\phi\,(\text{m/s}), \qquad R^2 = 0.788 \quad (5)$$

$$V_S = 3512 - 42.76\phi\,(\text{m/s}), \qquad R^2 = 0.763 \quad (6)$$

where ϕ is porosity (percentage) and R^2 is the correlation coefficient.

In oil/water-saturated samples at the same effective pressure and temperature (Figure 6b),

$$V_P = 6417 - 67.66\phi\,(\text{m/s}), \qquad R^2 = 0.891 \quad (7)$$

and

$$V_S = 3565 - 52.46\phi\,(\text{m/s}), \qquad R^2 = 0.853. \quad (8)$$

In CO_2 flooded samples (Figure 6c),

$$V_P = 6504 - 81.09\phi\,(\text{m/s}), \qquad R^2 = 0.881 \quad (9)$$

and

$$V_S = 3567 - 53.72\phi\,(\text{m/s}), \qquad R^2 = 0.874. \quad (10)$$

Interestingly, both V_P and V_S are more dependent on, and better correlated to, porosity in oil/water-saturated and CO_2-flooded samples than in dry (air-saturated) samples. This is because in dry rocks, seismic velocities are affected greatly by the presence of thin or flat pores. In liquid-saturated rocks, these thin pores are filled with a liquid, so they become less compressible and in turn have less effect on the velocities.

Table 3 lists all the measured velocities and calculated Poisson's ratios of the eight McElroy samples at the three saturation conditions (dry, oil/water saturated, and CO_2 flooded).

Effect of oil/water saturation

The effect of oil/water saturation is calculated by

$$\text{Effect of saturation} = \frac{\text{Oil/water saturated velocity} - \text{Dry velocity}}{\text{Dry velocity}} \times 100\%. \quad (11)$$

In general, V_P should increase and V_S should decrease as a porous rock is fully saturated with a liquid. In our measured McElroy samples under the original reservoir condition (overburden pressure = 2900 psi, pore pressure = 1200 psi, temperature = 88°F), the V_P increase ranges from 1.5% to as high as 12.4%, while the V_S decrease ranges from 1.8% to 7.2% as the samples are fully saturated with the oil/water mixture (about 60/40). In sample 11, V_S actually increases by 1% (Figure 7 and Table 3).

Effect of CO_2 flooding

The effects of CO_2 flooding on the velocities are calculated by

$$\text{Effect of flooding} = \frac{CO_2 \text{ flooded velocity} - \text{Oil/water saturated velocity}}{\text{Oil/water saturated velocity}} \times 100\%. \quad (12)$$

Table 2. Water and CO_2 displacement/saturation in McElroy carbonates.

				Water displacement					CO_2 flood			
Sample number	Porosity (%)	Permeability (md)	Pore volume (P.V.) (cm^3)	Water injected (cm^3)	Water injected (P.V.)	Oil displaced (cm^3)	Oil saturation (%)	Water saturation (%)	CO_2 injected (cc)	CO_2 injected (P.V.)	Final CO_2 saturation (%)	Final oil/water saturation (%)
1	12.0	1.08	6.32	45.8	7.2	2.51	60.3	39.72	41.8	6.6	53.91	46.09
5	21.4	53.10	11.32	86.9	7.7	5.01	55.7	44.26	94.4	8.3	76.44	23.56
6	21.7	53.90	10.57	97.0	9.2	5.51	47.9	52.13	92.1	8.7	62.67	37.33
7	13.7	16.90	7.07	69.3	9.8	2.51	64.5	35.50	86.3	12.2	62.79	37.21
8	22.1	66.70	11.84	84.7	7.2	5.51	53.5	46.54	86.6	7.3	66.95	33.05
9	12.3	2.56	5.58	58.2	10.4	2.01	64.0	36.02	75.3	13.5	69.55	30.45
11	7.9	0.40	3.64	368.0*	101.1*	1.01	72.3	27.75	81.2	22.3	59.69	40.31
12	8.2	0.07	3.74	17.4	4.7	1.21	67.6	32.35	81.2	21.7	51.76	48.24
Average	**14.91**	**24.34**	**7.51**	**65.61**	**8.02**	**3.16**	**60.72**	**39.28**	**79.86**	**12.59**	**62.97**	**37.03**

*Water breakthrough overnight. The average calculation did not count these figures.

CO_2 flooding decreases compressional velocities at all effective pressures (Figure 8a). The V_P decrease ranges from 0.2% to 8.7%, with the extent of the decrease being a strong function of porosity. The three high-porosity samples (5, 6, and 8) all show large V_P decreases after the oil/water-saturated samples are flooded with CO_2. The effect of CO_2 flooding on V_P in samples with low-to-medium porosities is quite small, with V_P decreases <2% (Table 3).

CO_2 flooding also decreases shear velocities in most cases (Figure 8b). At high effective pressures (low pore pressures), V_S shows a slight increase in samples 7 and 11. The V_S decrease ranges from 0.1% to 2.8% (Table 3).

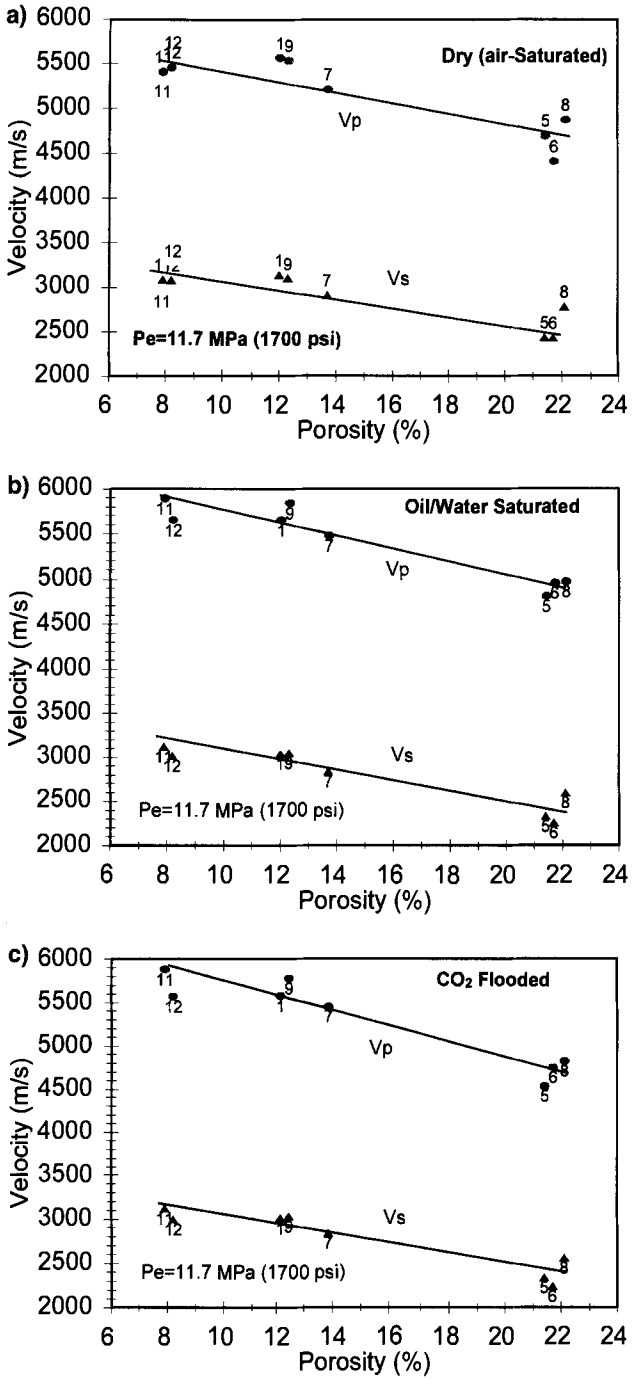

FIG. 6. Compressional (V_P) and shear (V_S) velocities versus porosity in gas-saturated (a), oil/water-saturated (b), and CO_2-flooded (c) samples of McElroy carbonate at original (before CO_2 flooding) reservoir conditions (net overburden pressure = 1700 psi or 11.7 MPa, temperature = 88°F or 31°C). Both V_P and V_S decrease approximately linearly with increasing porosity. Each data point is labeled with the sample number.

Effect of pressure

The effect of CO_2 flooding on V_P and V_S is dependent not only on porosity but also on either effective or pore pressure. The higher the pore pressure (or the lower the effective pressure) at a constant overburden pressure of 2900 psi (20 MPa), the larger the effect of CO_2 flooding (Figures 8a and 8b).

The effect of pressure on the velocities is calculated by

$$\text{Effect of pressure} = \frac{\text{Velocity}\big|_{P_p=2300\,\text{psi}}^{P_{ov}=2900\,\text{psi}} - \text{Velocity}\big|_{P_p=1200\,\text{psi}}^{P_{ov}=2900\,\text{psi}}}{\text{Velocity}\big|_{P_p=1200\,\text{psi}}^{P_{ov}=2900\,\text{psi}}} \times 100\%, \quad (13)$$

where P_{ov} and P_p are overburden and pore pressures, respectively.

Figure 9a shows the effect of pore pressure on V_P and V_S in oil/water-saturated samples. As the pore pressure increases from 1200 psi (8.3 MPa) to 2300 psi (15.9 MPa) at a constant overburden pressure of 2900 psi (20 MPa), V_P decreases 1.7–5.0% and V_S decreases 2.6–7.6% at the reservoir temperature of 88°F (31°C). In CO_2-flooded samples, the decreases are 2.0–6.9% for V_P and 3.1–8.5% for V_S (Figure 9b).

Note that V_S is more dependent on pore pressure (or effective pressure) than V_P. Furthermore, the pressure effect is larger in high-porosity samples (Figures 9a and 9b).

Figure 10 shows the combined effect of pore pressure increase (from 1200 to 2300 psi at a constant overburden pressure of 2900 psi) and CO_2 flooding on V_P and V_S in the measured

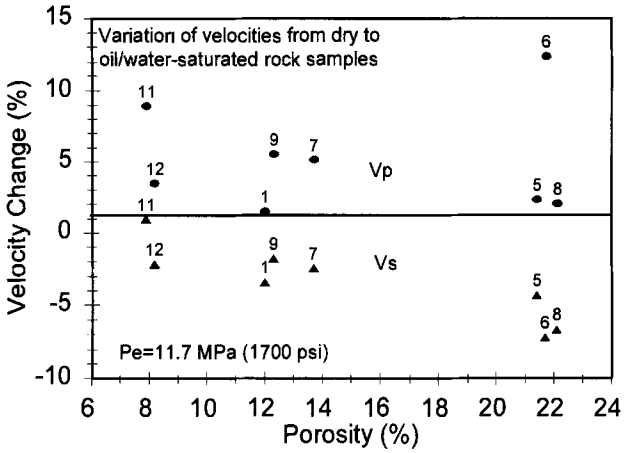

FIG. 7. Effect of oil/water saturation on V_P and V_S under the original McElroy reservoir conditions (before CO_2 flooding). The V_P increase ranges from 1.5% to as high as 12.4%, while the V_S decrease ranges from 1.8% to 7.2%, as the samples are fully saturated with the oil/water mixture (about 60/40). Each data point is labeled with the sample number.

core samples. Decreases in both V_P and V_S range from 3% to as high as 11%. Such decreases average around 9% in high-porosity samples and around 4% in low-to-medium porosity samples.

THEORETICAL CALCULATIONS

Gassmann (1951) derived an equation to calculate the bulk modulus of a fluid-saturated porous medium using the known bulk moduli of the solid matrix (grain), the frame, and the pore fluid. For a rock, the solid matrix consists of the rock-forming minerals, the frame refers to the rock sample with empty pores (dry rock), and the pore fluid can be a gas, oil, brine, or mixture:

$$K^* = K_d + \frac{(1 - K_d/K_m)^2}{\dfrac{\phi}{K_f} + \dfrac{1-\phi}{K_m} - \dfrac{K_d}{K_m^2}}, \tag{14}$$

where K^* is the bulk modulus of a rock saturated with a fluid of bulk modulus K_f, K_d is the frame (dry) bulk modulus, K_m is the matrix (grain) bulk modulus of the same rock, and ϕ is porosity. The shear modulus μ^* of the rock is not affected by fluid saturation, so

$$\mu^* = \mu_d, \tag{15}$$

where μ_d is the frame (dry) shear modulus of the rock. The density ρ^* of the saturated rock is given by

$$\rho^* = \rho_d + \phi\rho_f, \tag{16}$$

where ρ^* and ρ_d are the fluid-saturated and dry densities of the rock, respectively, and ρ_f is the pore fluid's density.

The Gassmann equation relates the fluid-saturated moduli to the known dry moduli and fluid properties. In other words, it permits calculation of the effect of fluid saturation on seismic velocities in rocks. It is a low-frequency approach, which means the calculated fluid-saturated velocities are of zero frequency.

For each of our eight core samples, we calculated the oil/water-saturated and CO_2-flooded velocities at all measured pressures using the measured dry (air-saturated) velocities, grain density, porosity, and fluid density and compressibility. We assumed the grain bulk modulus K_m in the Gassmann equation to have a linear empirical relationship with the grain density ρ_m:

$$K_m = 95 - 112.5(2.87 - \rho_m) \quad \text{(GPa)}. \tag{17}$$

Equation (17) yields a grain bulk modulus of 95 GPa for pure dolomite, whose density is 2.87 g/cm^3, and 77 GPa for pure calcite, whose density is 2.71 g/cm^3.

The bulk modulus K_f of the oil/water mixture is calculated using Wood's equation (Wood, 1941),

$$\frac{1}{K_f} = \frac{S_w}{K_w} + \frac{1 - S_w}{K_o}, \tag{18}$$

where K_w and K_o are the bulk moduli of brine and oil, respectively, and S_w is the brine saturation in fraction. Wood's equation is based on the uniform stress assumption for fluid mixtures.

Table 3. Measured velocity data in the McElroy cores, grouped by effective pressure.

	300 psi			600 psi			900 psi			1300 psi			1700 psi		
Sample number	V_P (m/s)	V_S (m/s)	Poisson's ratio	V_P (m/s)	V_S (m/s)	Poisson's ratio	V_P (m/s)	V_S (m/s)	Poisson's ratio	V_P (m/s)	V_S (m/s)	Poisson's ratio	V_P (m/s)	V_S (m/s)	Poisson's ratio
Dry (air-saturated) rocks															
1	5406	3080	0.260	5449	3096	0.262	5486	3108	0.264	5531	3125	0.266	5566	3143	0.266
5	4475	2346	0.311	4545	2381	0.311	4492	2401	0.300	4648	2423	0.313	4702	2440	0.316
6	3902	2204	0.266	4022	2260	0.269	4131	2318	0.270	4275	2388	0.273	4416	2439	0.281
7				5096	2804	0.283	5122	2833	0.280	5164	2875	0.275	5214	2913	0.273
8				4777	2684	0.269	4822	2712	0.269	4852	2749	0.264	4878	2787	0.258
9				5402	3061	0.264	5439	3070	0.266	5487	3087	0.268	5534	3103	0.271
11	5158	2933	0.261	5203	2977	0.257	5258	3008	0.257	5329	3054	0.255	5411	3090	0.258
12	5371	3040	0.264	5387	3052	0.264	5403	3063	0.263	5429	3071	0.265	5460	3081	0.266
Oil/water-saturated rocks															
1	5456	2874	0.308	5532	2933	0.304	5582	2974	0.302	5626	3014	0.299	5650	3036	0.297
5	4577	2153	0.358	4648	2225	0.351	4708	2272	0.348	4765	2312	0.346	4811	2335	0.346
6	4606	2035	0.379	4714	2090	0.378	4804	2145	0.375	4902	2221	0.371	4962	2263	0.369
7				5356	2760	0.319	5389	2793	0.316	5438	2823	0.316	5482	2842	0.316
8	4758	2389	0.331	4822	2461	0.324	4884	2509	0.321	4948	2563	0.317	4976	2601	0.312
9				5733	2966	0.317	5775	2994	0.316	5817	3026	0.314	5841	3048	0.313
11	5670	2944	0.315	5748	2998	0.313	5809	3048	0.310	5865	3096	0.307	5895	3120	0.305
12	5500	2891	0.309	5556	2935	0.306	5592	2965	0.304	5628	2996	0.302	5650	3014	0.301
CO_2-flooded rocks															
1	5360	2852	0.303	5446	2907	0.301	5504	2947	0.299	5545	2984	0.296	5576	3011	0.294
5	4179	2093	0.333	4315	2205	0.323	4411	2262	0.322	4469	2306	0.319	4528	2334	0.319
6	4281	1984	0.363	4419	2047	0.363	4547	2117	0.362	4665	2201	0.357	4747	2238	0.357
7				5288	2747	0.315	5343	2785	0.313	5395	2822	0.312	5456	2845	0.313
8	4511	2335	0.317	4609	2394	0.315	4689	2437	0.315	4761	2499	0.310	4821	2554	0.305
9				5634	2940	0.313	5694	2979	0.312	5738	3007	0.311	5778	3032	0.310
11	5624	2896	0.320	5719	2973	0.315	5786	3036	0.310	5842	3092	0.305	5882	3122	0.304
12	5393	2867	0.303	5461	2906	0.302	5502	2937	0.301	5546	2976	0.298	5570	2999	0.296

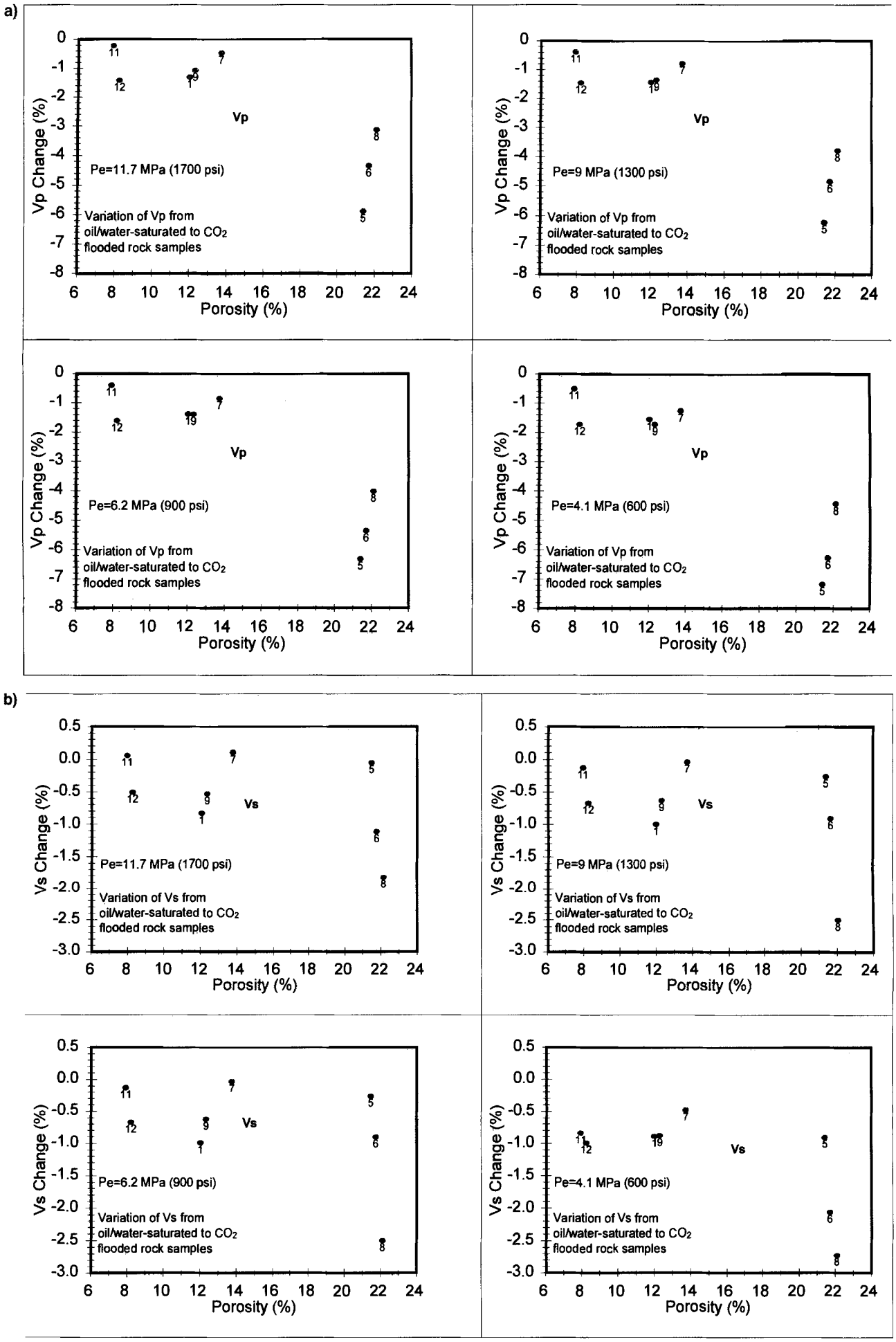

FIG. 8. Effect of CO_2 flooding on V_P (a) and V_S (b) at different net overburden pressures (Pe). CO_2 flooding decreases V_P at all effective pressures. The V_P decrease ranges from 0.2% to 8.7% and is a strong function of porosity. CO_2 flooding also decreases V_S in most samples. Each data point is labeled with the sample number.

The bulk modus K_{fc} of the CO_2 and oil/water mixture after the rock is flooded with CO_2 can also be calculated using Wood's equation:

$$\frac{1}{K_{fc}} = \frac{S_{CO_2}}{K_{CO_2}} + \frac{1 - S_{CO_2}}{K_f}, \quad (19)$$

where K_{CO_2} and K_f are the bulk moduli of CO_2 and oil/water, respectively, and S_{CO_2} is the CO_2 saturation in fraction. Note that the uncertainties in the measured saturations, estimated to be within ±5% saturation unit, are transferred to the calculated bulk modulus of the fluid mixtures.

The calculated V_P values using the Gassmann equation are in general lower than the laboratory-measured V_P values in either the oil/water-saturated or CO_2-flooded samples, whereas the Gassmann-calculated V_S values are slightly higher than the laboratory-measured V_S values at all pressures (Table 4).

DISCUSSION

The feasibility of using seismic methods to monitor CO_2 flooding in situ depends on at least two major factors: the resolution of the seismic method and the effect of CO_2 flooding on seismic properties of reservoir rocks. Traditional seismic tomography measures the direct arrival velocity or traveltime difference before and after CO_2 flooding, while surface 3-D monitoring measures the reflected time difference and the impedance contrast. The high-resolution crosswell tomography applied to the McElroy data can resolve as little as 1% velocity change (Harris et al., 1995).

The effect of CO_2 flooding on seismic properties depends on many factors, such as the compressibility contrast between the pore fluids before and after flooding, the pore structure of the reservoir rock, the injection pressure and reservoir pressure buildup, and formation temperature. Furthermore, these factors are interactive: as one factor changes, almost all others will change. In this section, we briefly discuss some main factors that affect the monitoring of CO_2 flooding seismically. For discussion purposes and clarity, we discuss these factors separately.

Effect of pore fluid change

Our results show that the effect of CO_2 flooding on V_P ranges from −0.2% to −8.7% (Table 5). This change is mostly caused by the compressibility contrast between CO_2 and the oil/water mixture in the reservoir. In general, the average effect of CO_2 flooding on V_P can be predicted using the Gassmann equation, although the Gassmann equation seems to be inadequate for some samples (Table 5).

The Gassmann-calculated CO_2 effect is the difference between Gassmann-calculated velocities in oil/water-saturated and CO_2-flooded rocks. The measured CO_2 effect on V_P is very close to that predicted by the Gassmann equation in most of the samples (except sample 5). The average measured CO_2 effect on V_P matches remarkably well with that calculated by the Gassmann equation. The Gassmann equation predicts that V_S is essentially unchanged by CO_2 flood, while the measured data show that V_S decreases by approximately 1%.

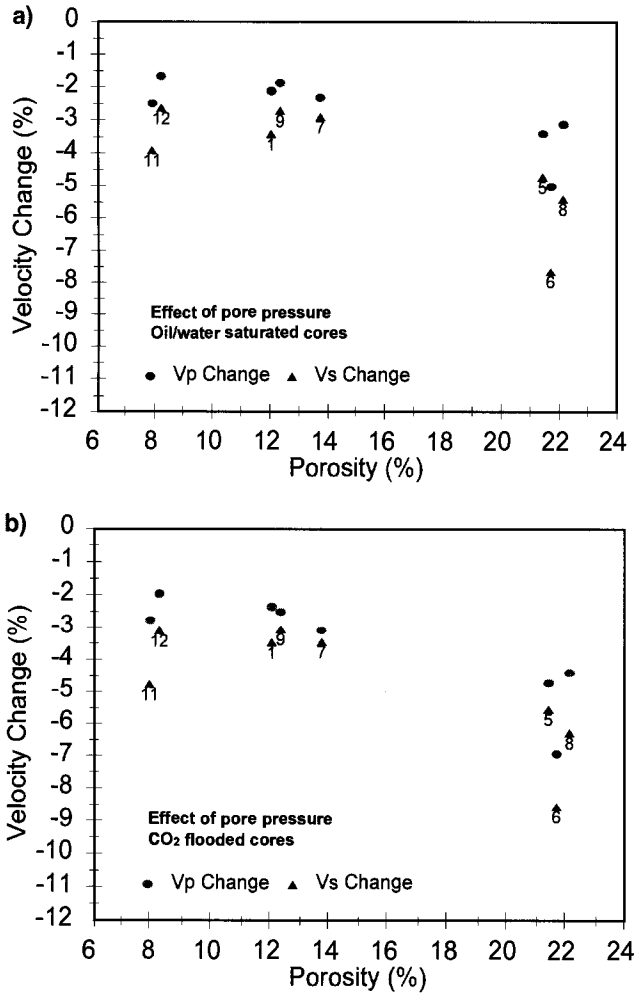

FIG. 9. Effect of pore pressure (increasing from 1200 psi or 8.3 MPa to 2300 psi or 15.9 MPa at a constant overburden pressure of 2900 psi or 20 MPa) on V_P and V_S in oil/water-saturated (a) and CO_2-flooded (b) samples. V_P decreases by 1.7% to 5.0% and V_S decreases by 2.6% to 7.6% in oil/water-saturated samples. In CO_2-flooded samples, the decreases are 2.0–6.9% for V_P and 3.1–8.5% for V_S. Each data point is labeled with the sample number.

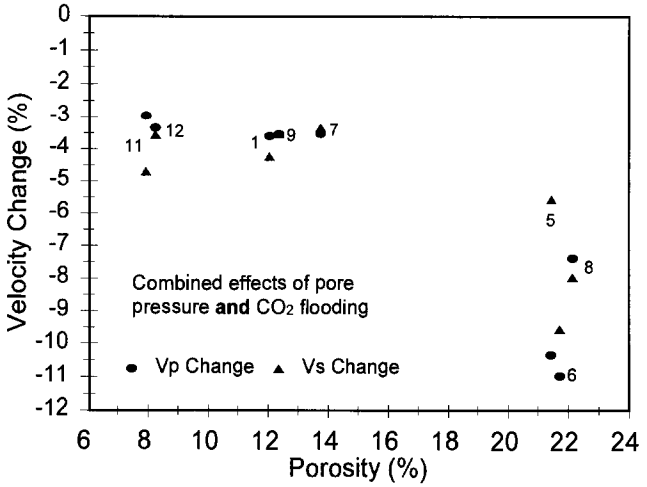

FIG. 10. Combined effects of CO_2 flooding or CO_2 saturation and pore pressure (increasing from 1200 psi or 8.3 MPa to 2300 psi or 15.9 MPa at a constant overburden pressure of 2900 psi or 20 MPa) on V_P and V_S in the McElroy samples. The V_P and V_S decreases caused by the CO_2 injection range from 3% to as high as 11%. Such decreases average 9% in high-porosity samples and 4% in low- to medium-porosity samples. Each data point is labeled with the sample number.

The laboratory-measured effect of CO_2 flooding on V_S ranges from −0.6% to −1.8% when averaged over all the measured samples. In theory, fluid substitution changes V_S only through the bulk density change because fluids do not affect the overall shear modulus of the rock. Since the bulk densities of CO_2 and reservoir oil/water are very comparable under reservoir conditions, CO_2 flooding in theory should not change V_S, as predicted by the Gassmann equation. In reality, fluids do affect the shear modulus of porous rocks through their wettability, viscosity, and perhaps other physicochemical factors.

Effect of reservoir depth and injection pressure

Shallow reservoirs are good candidates for seismic monitoring because seismic velocities are more sensitive to pore fluid changes under lower effective pressures. The McElroy

Table 4. Calculated velocities using the Gassmann equation.

Oil/water saturated	300 psi		600 psi		900 psi		1300 psi		1700 psi	
Sample number	V_P^* (m/s)	V_S^* (m/s)	V_P^* (m/s)	V_S^* (m/s)	V_P^* (m/s)	V_S^* (m/s)	V_P^* (m/s)	V_S^* (m/s)	V_P^* (m/s)	V_S^* (m/s)
1V	5460	3014	5494	3029	5523	3041	5559	3058	5587	3076
5V	4491	2248	4548	2281	4505	2301	4630	2322	4673	2338
6V	4030	2111	4124	2164	4211	2220	4327	2287	4440	2336
7V			5138	2733	5160	2761	5196	2802	5238	2839
8V			4751	2568	4788	2595	4813	2630	4835	2667
9V			5431	2992	5460	3000	5498	3017	5535	3033
11V	5345	2892	5382	2936	5424	2967	5480	3012	5542	3048
12V	5490	2996	5502	3007	5514	3018	5532	3026	5554	3036
CO_2 flooded										
1V	5334	3015	5371	3032	5403	3044	5442	3062	5480	3088
5V	4341	2250	4403	2285	4351	2305	4493	2328	4555	2357
6V	3812	2113	3917	2167	4013	2224	4141	2294	4280	2355
7V			5008	2735	5030	2764	5066	2807	5119	2853
8V			4616	2572	4655	2599	4681	2638	4719	2689
9V			5317	2994	5349	3003	5392	3022	5442	3046
11V	5154	2894	5191	2937	5237	2968	5296	3015	5368	3056
12V	5344	2997	5355	3009	5366	3020	5384	3029	5410	3045

Table 5. Effect of CO_2 flooding on oil/water-saturated cores, grouped by effective pressure.

Calculated using the laboratory-measured data		300 psi		600 psi		900 psi		1300 psi		1700 psi	
Sample number	Porosity (%)	V_P (%)	V_S (%)	V_P (%)	V_S (%)	V_P (%)	V_S (%)	V_P (%)	V_S (%)	V_P (%)	V_S (%)
1	12.0	−1.76	−0.77	−1.55	−0.89	−1.40	−0.91	−1.44	−1.00	−1.31	−0.82
5	21.4	−8.70	−2.79	−7.16	−0.90	−6.31	−0.44	−6.21	−0.26	−5.88	−0.04
6	21.7	−7.06	−2.51	−6.26	−2.06	−5.35	−1.31	−4.83	−0.90	−4.33	−1.10
7	13.7			−1.27	−0.47	−0.85	−0.29	−0.79	−0.04	−0.47	0.11
8	22.1	−5.19	−2.26	−4.42	−2.72	−3.99	−2.87	−3.78	−2.50	−3.11	−1.81
9	12.3			−1.73	−0.88	−1.40	−0.50	−1.36	−0.63	−1.08	−0.52
11	7.9	−0.81	−1.63	−0.50	−0.83	−0.40	−0.39	−0.39	−0.13	−0.22	0.06
12	8.2	−1.95	−0.83	−1.71	−0.99	−1.61	−0.94	−1.46	−0.67	−1.42	−0.50
Average All	**14.91**	**−4.24**	**−1.80**	**−3.08**	**−1.22**	**−2.66**	**−0.96**	**−2.53**	**−0.76**	**−2.23**	**−0.58**
Average 1	*21.73*	*−6.98*	*−2.52*	*−5.95*	*−1.89*	*−5.22*	*−1.54*	*−4.94*	*−1.22*	*−4.44*	*−0.98*
Average 2	**10.82**	**−1.51**	**−1.08**	**−1.35**	**−0.81**	**−1.13**	**−0.61**	**−1.09**	**−0.49**	**−0.90**	**−0.34**
Calculated using the Gassmann equation											
1	12.0	−2.31	0.06	−2.23	0.07	−2.17	0.09	−2.10	0.15	−1.91	0.41
5	21.4	−3.34	0.11	−3.19	0.14	−3.44	0.17	−2.96	0.28	−2.52	0.80
6	21.7	−5.40	0.11	−5.02	0.15	−4.71	0.18	−4.29	0.28	−3.60	0.81
7	13.7			−2.53	0.09	−2.53	0.11	−2.50	0.17	−2.27	0.49
8	22.1			−2.84	0.15	−2.78	0.18	−2.74	0.29	−2.40	0.83
9	12.3			−2.10	0.08	−2.03	0.10	−1.93	0.15	−1.68	0.44
11	7.9	−3.57	0.04	−3.54	0.05	−3.45	0.06	−3.35	0.09	−3.15	0.27
12	8.2	−2.66	0.04	−2.67	0.05	−2.69	0.06	−2.67	0.10	−2.60	0.28
Average All	**14.91**	**−3.45**	**0.07**	**−3.02**	**0.10**	**−2.97**	**0.12**	**−2.82**	**0.19**	**−2.52**	**0.54**
Average 1	*21.73*	*−4.37*	*0.11*	*−3.68*	*0.15*	*−3.64*	*0.18*	*−3.33*	*0.29*	*−2.84*	*0.82*
Average 2	**10.82**	**−2.84**	**0.04**	**−2.62**	**0.07**	**−2.57**	**0.08**	**−2.51**	**0.13**	**−2.32**	**0.38**

Average All: Averaged over all samples.
Average 1: Averaged over high-porosity, high-permeability samples.
Average 2: Averaged over low-to-medium porosity, low-permeability samples.

reservoir depth is <3000 ft (914 m), which is quite shallow. Because of its relatively low overburden pressure (approximately 2900 psi or 20 MPa), the effect of formation pressure buildup caused by the CO_2 injection is large. In-situ measurements of bottom-hole pressures after CO_2 injection showed a formation pressure of 2300 psi to as high as 2600 psi (15.9 to 17.9 MPa). Such high pore pressures yield net or effective reservoir pressures of only 300 to 600 psi (2.1 to 4.1 MPa).

The high formation pore pressure buildup (pore pressure increases from 1200 to 2300 psi at a constant overburden pressure of 2900 psi) decreases both V_P and V_S. The average V_P and V_S decreases range from 2.7% to 4.8%, respectively (Table 6). The average V_P decrease is again predicted well by the Gassmann equation. The measured V_S decrease is higher than that calculated by the Gassmann equation.

Separating pore pressure effect from CO_2 effect

In-situ crosswell seismic surveys measure the combined effects of CO_2 saturation and pore pressure increase on velocities. Table 7 shows the combined effects of CO_2 flooding and pore pressure increase on V_P and V_S as measured in the laboratory and calculated by the Gassmann equation. The data reveal we might be able to decouple, at least semiquantitatively, these two effects using our laboratory results. Compared to V_P, V_S is much less affected by CO_2 saturation: the laboratory results show slight decreases in V_S as the samples are flooded with CO_2 (at constant overburden and pore pressures), while the Gassmann equation predicts slight increases. In contrast, V_S is more sensitive to pore pressure changes than V_P. As a result, a large portion of the measured total decreases in V_S by seismic surveys before and after CO_2 flooding is caused by pore pressure increases.

The mechanism for V_S being more sensitive to pore pressure changes than V_P is related to the properties of CO_2. As pore pressure increases, both the bulk modulus and bulk density of CO_2 increase considerably. In a CO_2-flooded rock, increase in pore pressure not only opens some originally closed thin pores or fractures, but it also increases the bulk density of the rock and the bulk modulus of the pore fluid. The effects of the bulk density increase and pore opening on the V_P in the CO_2-flooded rock are offset partially by the effect of bulk modulus increase

Table 6. Effect of pore pressure (1200–2300 psi) at a constant overburden pressure of 2900 psi.

			Oil/water-saturated cores				CO_2-flooded cores			
			Measured		Gassmann		Measured		Gassmann	
Sample number	Porosity (%)	Perm (md)	V_P (%)	V_S (%)	V_P (%)	V_S (%)	V_P (%)	V_S (%)	V_P (%)	V_S (%)
1	12.0	1.08	−2.09	−3.39	−1.67	−1.50	−2.33	−3.45	−1.99	−1.84
5	21.4	53.10	−3.39	−4.71	−2.68	−2.44	−4.70	−5.53	−3.34	−3.07
6	21.7	53.90	−5.00	−7.64	−7.11	−7.36	−6.91	−8.53	−8.49	−7.97
7	13.7	16.90	−2.30	−2.89	−1.90	−3.75	−3.08	−3.44	−2.16	−4.14
8	22.1	66.70	−3.09	−5.38	−1.75	−3.71	−4.40	−6.26	−2.19	−4.36
9	12.3	2.56	−1.85	−2.69	−1.89	−1.36	−2.49	−3.03	−2.31	−1.71
11	7.9	0.40	−2.49	−3.91	−2.89	−3.66	−2.77	−4.77	−3.28	−3.87
12	8.2	0.07	−1.66	−2.62	−0.93	−0.95	−1.96	−3.10	−1.01	−1.18
Average All	**14.91**	**24.34**	**−2.73**	**−4.15**	**−2.60**	**−3.09**	**−3.58**	**−4.77**	**−3.10**	**−3.52**
Average 1	*21.73*	*57.90*	*−3.83*	*−5.91*	*−3.85*	*−4.50*	*−5.34*	*−6.78*	*−4.67*	*−5.14*
Average 2	**10.82**	**4.20**	**−2.08**	**−3.10**	**−1.86**	**−2.25**	**−2.53**	**−3.56**	**−2.15**	**−2.55**

Average All: Averaged over all samples.
Average 1: Averaged over high-porosity, high-permeability samples.
Average 2: Averaged over low-to-medium porosity, low-permeability samples.

Table 7. Combined effects of CO_2 saturation and pore pressure change. Overburden pressure = 2900 psi; pore pressure from 1200 to 2300 psi.

			Measured		Gassmann	
Sample number	Porosity (%)	Permeability (md)	V_P (%)	V_S (%)	V_P (%)	V_S (%)
1	12.0	1.08	−3.61	−4.25	−3.86	−1.43
5	21.4	53.10	−10.31	−5.57	−5.78	−2.30
6	21.7	53.90	−10.94	−9.54	−11.78	−7.22
7	13.7	16.90	−3.54	−3.34	−4.38	−3.67
8	22.1	66.70	−7.38	−7.96	−4.54	−3.57
9	12.3	2.56	−3.54	−3.54	−3.95	−1.29
11	7.9	0.40	−2.99	−4.71	−6.33	−3.62
12	8.2	0.07	−3.35	−3.58	−3.58	−0.90
Average All	**14.91**	**24.34**	**− 5.71**	**−5.31**	**− 5.53**	**−3.00**
Average 1	*21.73*	*57.90*	*− 9.54*	*−7.69*	*− 7.37*	*−4.36*
Average 2	**10.82**	**4.20**	**− 3.40**	**−3.89**	**− 4.42**	**− 2.18**

Average All: Averaged over all samples.
Average 1: Averaged over high-porosity, high-permeability samples.
Average 2: Averaged over low-to-medium porosity, low-permeability samples.

in the pore fluid. Because fluids do not support shear stresses, the effects of the bulk density increase and pore-opening on V_S in the CO_2-flooded rock are not offset by anything.

In practice, V_P alone is inadequate as a CO_2/pore pressure discriminator because both CO_2 saturation and increase in pore pressure decrease V_P. Because V_S is insensitive to CO_2 saturation, but sensitive to pore pressure increase, it is a good CO_2/pore pressure discriminator. If a zone shows large V_P decrease but little V_S change, it is very likely swept by CO_2 at a pore pressure near the original (before CO_2 flooding) reservoir pore pressure. On the other hand, if a zone shows large decreases in V_P and V_S, it is probably swept by CO_2 with pore pressure buildup.

Seismic delineation of flow heterogeneity

Three types of averages of data are calculated in Tables 5, 6, and 7: Average All, Average 1, and Average 2. Average All is the average of all the eight samples; Average 1 is the average of the high-porosity, high-permeability samples (5, 6, and 8); and Average 2 is the average of the rest of the samples (samples 1, 7, 9, 11, and 12, with low-to-medium porosities and low permeabilities).

V_P and V_S changes are four and three times, respectively, greater in high-porosity, high-permeability samples than those in low-to-medium porosity, low-permeability samples because of CO_2 flooding. Both V_P and V_S are twice as sensitive to pore pressure changes in high-porosity, high-permeability samples than in low-to-medium porosity, low-permeability samples because of pore pressure increases. In terms of the combined effects of CO_2 saturation and pore pressure buildup, V_P and V_S decrease 9.5% and 7.7%, respectively, in high-porosity, high-permeability samples (Average 1), while they decrease only 3.4% and 3.9%, respectively, in low-to-medium porosity, low-permeability (Average 2) samples (Table 7).

Because CO_2 flooding and pore pressure buildup decrease V_P and V_S more in high-porosity, high-permeability samples, it may be possible to delineate such high-porosity, high-permeability streaks seismically in situ. If the streaks are thick enough compared to seismic resolution, they can be identified by the larger V_P or V_S changes.

CONCLUSION

Our laboratory results show that under CO_2 injection conditions in the McElroy field, CO_2 has essentially the density of the reservoir oil and the bulk modulus of a compressed gas. As CO_2 displaces the original reservoir fluid, an oil/water mixture, it decreases the bulk modulus with little change in the bulk density of the reservoir rock. As a result, V_P in the reservoir decreases. Our laboratory results show that the effect of CO_2 flooding alone (not counting other effects such as pore pressure change) decreases V_P on average 2–4% and up to 9% in high-porosity rocks. CO_2 flooding also decreases V_S, typically 0.5–2%. The magnitude of the V_P decrease can certainly be resolved by high-resolution seismic surveys, especially crosswell tomographic imaging, where the traveltime reproducibility is around 1% in the surveys.

Because CO_2 must be injected at a higher pressure than the original formation pore fluid pressure, CO_2 injection decreases the effective or differential reservoir pressure. As a result, both V_P and V_S in the reservoir decrease. Our laboratory and theoretical results show that the effect of pore fluid pressure alone (from the preinjection formation pore pressure of 1200 psi to the postinjection formation pore pressure of 2300 psi) decreases V_P by an average of 3% and V_S by 4%. Again, the velocity decreases caused by the pore pressure change alone may be resolved by high-resolution seismic surveys.

Both the injected CO_2 and high injection pressure decrease the seismic velocities in the reservoir. The two effects are almost additive, so the combined effects of CO_2 flooding and increase in pore pressure decrease V_P by an average of 6% and V_S by 5%. In high-porosity samples, the V_P and V_S decreases can be as high as 11% and 10%, respectively.

In addition to the effects of CO_2 saturation and pore pressure change, other factors in the McElroy field are also in favor of monitoring the CO_2 flood process seismically. First, the reservoir is relatively shallow [about 2900 ft (884 m)], so seismic velocities are more sensitive to pore pressure and pore fluid changes. Because of the shallow depth, the increase of formation pore pressure from 1200 psi to 2300 psi decreases the effective reservoir pressure from 1700 psi to 600 psi. At low effective reservoir pressures, the rock frame is softer, so V_P is more sensitive to pore fluid change. Second, the reservoir temperature is relatively low (88°F or 31°C) so the injected CO_2 has a bulk density comparable to that of the original reservoir fluids (oil and water), whereas it is nearly 10 times more compressible than the original reservoir fluids.

Field results of time-lapse crosswell tomographic imaging have shown that both V_P and V_S decrease as a result of CO_2 injection. Such decreases can be as high as 10%. Our laboratory results confirm that V_P and V_S can indeed decrease by 10% in some high-porosity reservoir rocks.

Although the Gassmann equation does not adequately predict the effect of oil/water saturation on V_P and V_S, it does predict similar average V_P and V_S decreases caused by the combined effects of CO_2 flooding and pore pressure change, as compared with our laboratory data. In other words, although the Gassmann-calculated data do not match the experimental data in terms of absolute V_P and V_S values, the calculated and measured average effects of CO_2 saturation and pore pressure change are comparable. For V_S, the Gassmann equation shows almost no change, while the measured data show slight decreases, as a result of CO_2 flooding alone.

Because V_S is insensitive to CO_2 saturation and sensitive to pore pressure increase, it is a good CO_2/pore pressure discriminator. In essence, V_S can be used, at least semiquantitatively, to separate CO_2-flooded zones with pore pressure buildup from those without pore pressure buildup.

Our results also reveal that high-porosity, high-permeability rocks are more sensitive to either CO_2 flooding or pore pressure increase, and time-lapse seismic survey results may be used to delineate such high-porosity, high-permeability streaks in the McElroy reservoir.

ACKNOWLEDGMENTS

The authors thank Ken Eisenmenger and Joe Stefani of Chevron for reviewing the manuscript; Mike Batzle, Pat Berge, and David Lumley for their constructive reviews; and Chevron Petroleum Technology Company for approving the publication of this paper.

REFERENCES

Batzle, M. L., and Wang, Z., 1992, Seismic properties of pore fluids: Geophysics, **57**, 1396–1408.

Gassmann, F., 1951, Uber die elastizitat poroser medien: Vertel-jahrsschrift der Naturforschenden Gesellschaft in Zurich, **96**, 1–23.

Harris, J. M., Nolen-Hoeksema, R. C., Langan, R. T., van Schaack, M., Lazaratos, S. K., and Rector, J. W., III, 1995, High-resolution cross-well imaging of a West Texas carbonate reservoir: Part 1—Project summary and interpretation: Geophysics, **60**, 667–681.

Lazaratos, S. K., and Marion, B. P., 1996, Crosswell seismic imaging of reservoir changes caused by CO_2 injection: 66th Ann. Internat. Mtg., Soc. Expl. Geophys., Expanded Abstracts, 1871–1879.

Nolen-Hoeksema, R. C., Wang, Z., Harris, J. M., and Langan, R. T., 1995, High-resolution crosswell imaging of a West Texas carbonate reservoir: Part 5—Core analysis: Geophysics, **60**, 712–726.

Wang, Z., Hirsche, K. W., and Sedgwick, G., 1991, Seismic velocities in carbonate rocks: J. Can. Petr. Tech., **30**, 112–122.

Wang, Z., and Nur, A., 1989, Effect of CO_2 flooding on wave velocities in rocks with hydrocarbons: Soc. Petr. Eng. Res. Eng., **3**, 429–439.

Wood, A. B., 1941, A textbook of sound: G. Bell and Sons.